Straight Line Aerodynamics Simulation of a FSAE Open-Wheel Car

Hugues PERRIN
Department of Aerospace Engineering, École de technologie supérieure, Montréal, Canada

Eline HOURI
Department of Aerospace Engineering, École de technologie supérieure, Montréal, Canada

Abstract

This work aims to detail the development of a straight line simulation model (SLSM) for aerodynamic analysis of a FSAE, open-wheel prototype. SLSM is the simpler approach widely used to study aerodynamics for its ease of setup and simplicity of correlation to on track data and wind tunnel testing. This paper will approach the basics of CFD and will detail how and why this model was created, used and validated.

NB : this paper is a proper re-edition of the collaborative work involving Eline Houri, for her Final Year Project (MGA961) at ÉTS, and Hugues Perrin, for his Research Project (TX51) at UTBM.. References about the literature review [1] and cornering simulation [2] are part of this re-edition.

Introduction

Designing aerodynamics devices for race cars, open-wheel prototypes in this instance, proves very technical work involving intense research and development cycles coupled with precise testing. Before Computational Fluid Dynamics (CFD) and Finite Element Analysis (FEA) codes entered an industrial context, innovative engineering was costly both financially and in terms of time as it implied design, fabrication and testing only to determine the efficiency of a newer part. The 1980s marked a leap in engineering design with the first simulation codes that allowed for the iteration of new parts without the necessity of fabrication, cutting costs in the R&D processes. [3]

The first CFD codes focused on internal aerodynamics for engine design and optimization [4] before scaling to 2D external aerodynamics and then 3D RANS over full cars with the increasing in computing power with the advent of High Performance Computing (HPC) and parallelization [5].

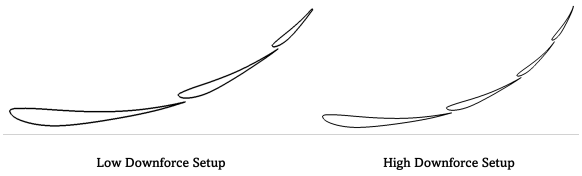

Figure 1: Front Wing profiles for initial 2D aerodynamic simulation

In the context of Formula SAE, Formula Student and modern open-wheel racing, characterization of aerodynamic effects is key to deliver a performative race car, whether its used is focused on stability, cornering speed (downforce production) or straight line speed (drag reduction). With innovation driving performance, it is critical the teams have a way to iterate designs faster and faster to ensure positive outcomes for the event, optimizing their car for each section of each track of the calendar. As such, each team of each category as a way of approaching and designing aerodynamic devices, with tools such as FEA and CFD, towards what engineers think is the best compromise, leading to sometimes small differences that account for the tenth of a second per lap differences between cars.

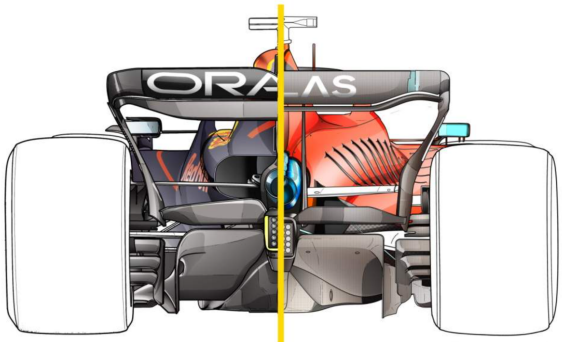

Figure 2: Comparison of the rear section of the RB18 (high downforce setup) and SF-75 (low downforce setup) cars during the 2022 Italian Grand Prix at Monza © TheRace

Since the 2010s, Formule ETS has been developing aerodynamic devices to increase the performance of their open-wheel prototype by implementing CFD in their design loops and quantifying the gains both in simulation and in real conditions. Those simulation started out as 2D evaluations of profile efficiency and interaction within multi-element wings which quickly evolved into 3D RANS simulations of isolated elements, and full car aerodynamics. In this context, straight line simulation models (SLSM) were used to quickly evaluate different design ideas in a reduced amount of time, taking advantage of the optimization and automatization features of more recent CFD softwares.

In 2023, Formule ETS carried-on their first Wind Tunnel correlation campaign to detect potential defaults in modeling and increase their understanding of the aerodynamics involved in the 10 to 20% gains in lap time.

This work will present the SLSM simulation techniques in CFD currently in use in Formule ETS to develop new appendages that increase performance by increasing downforce, lowering drag, bettering stability or making the cooling more reliable.

Modeling of the Case

The modeling of the straight line simulation case will regroup three sub-categories, being the geometry of the object and the domain of simulation, the discretization of those geometries into meshes and the physics equations that will be solved on that mesh.

Simplification of the Geometry

The outside geometry of a car, let alone a race car, can be very complex and detailed, including lots of smaller features like joint slots, screw heads, cables or sensors that could interfere with the flow. As a first step, it is crucial to simplify the geometry of the car by deciding which feature are negligible and which ones are crucial and have to be meshed.

In the case of Formule ETS' MANIC-24, a separate CAD assembly was made to replicate every outside geometry such as the front and rear wings, the undertray, the monocoque and the wheels of the manufactured car. This allows for a cleaner implementation into a CFD software while also streamlining the creation of new design iterations. This assembly is considered perfectly symmetrical, hence why only the left part of the car is modeled.

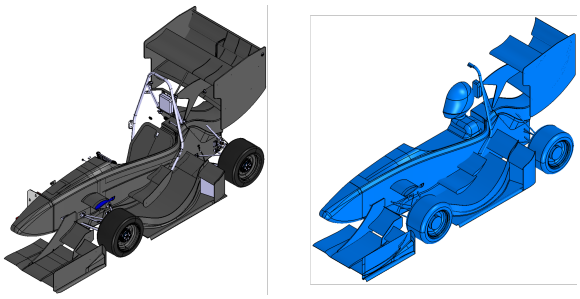

Figure 3: Comparison between the general CAD (left) and the CFD CAD (right)

The suppressed elements include routing cables along the suspension, bolt heads, brackets and generaly any feature that is significantly smaller than the ones around it. Any part not in direct contact with external air like the High-Voltage bay or the inside of the chassis are not modeled. A mannequin is added to replicate the presence of a driver in running condition.

The CFD CAD is organized as such :

- **01. CFD Chassis** : regroups every fixed part tied to the chassis and other departments (*Monocoque, Mannequin, Mainhoop, Head Rest, Suspension Links, TSAL, Keel, Rear Cover*)
- **02. CFD Wheels** : simplified geometry of the drivetrain assembly including tyres, wheel rims, gearbox covers and all rotating elements (*Front Wheel, Rear Wheel*)
- **03. CFD Front Wing** : aerodynamic devices located forwards of the front wheels (*Mainplane, Main Flap, Auxiliary Flap, Inboard/Middle/Outboard Endplate*)
- **04. CFD Rear Wing** : aerodynamic devices located upwards of the rear axle (*Mainplane, First/Second/Top Flaps, Endplate, Swan Neck*)
- **05. CFD Side Wing** : aerodynamic devices located on the top side of the car (*Top Wheel, Side Main, Side Flap, Undertray Flap*)
- **06. CFD Undertray** : aerodynamic devices located on the bottom side of the car, generally associated with ground effect (*Undertray, Bargeboard*)
- **07. CFD Cooling** : every cooling related components (*Cooling Housing, Cooling Flap, Radiator*)

The figure 4 is a visual representation of these sub-assemblies.

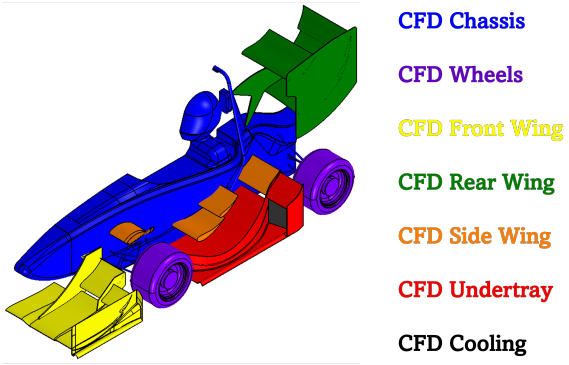

Figure 4: Organization and CFD implementation of the CFD CAD

The assembly is imported as is in StarCCM via the built-in plugins for CAD import. Singular parts or sub-assemblies can be easily replaced with new designs to test without re-importing or modifying other assemblies, granting ease of use and productivity.

To each part of each sub-assemblies is assigned a specific region and boundary condition (typically a smooth, no-slip wall). The break down in multiple region allows for an easier per-part summary of aerodynamic forces and an overall better comprehension of each innovation's influence.

The radiator is defined as a porous region with specific, measured, inertial and viscous resistances. This porous region interacts with the main fluid region through two interfaces, namely the inlet and outlet of the radiator.

Domain Definition

The domain is the continuous environment (in this case a rectangular box) that represents where the fluid can flow freely depending on the domain's boundary conditions and involved geometries.

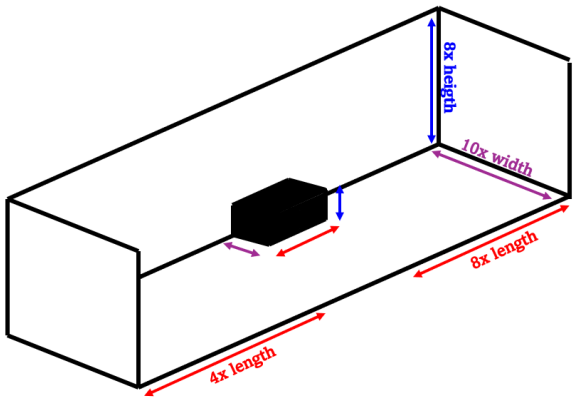

Figure 5: Final sizing of the CFD domain

The aerospace general rule of thumb for domain sizing is about making the domain large enough that flow returns to the initial freestream condition at the limits of the domain. However, for low-speed subsonic flows, the influence of the domain size is significantly reduced compared to compressible flows which allows for a smaller mesh, and faster computing. In our case, we settled on an approximately 6 x 20 x 10 meters box, where all the size are multiples of the car's dimensions.

A quick study was led to determine domain independence of the solution. In this study, different mesh sizes were computed with exact same car geometries, mesh algorithm and physics.

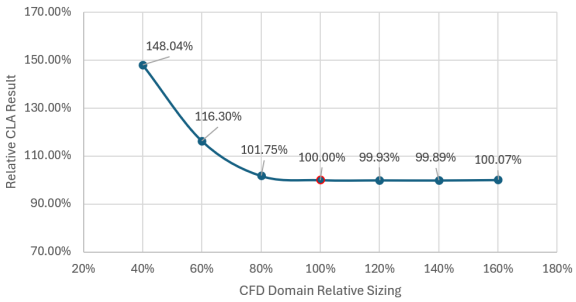

Figure 6: Validation of the mesh sizing and domain size independence

NB : All results are kept as relatives for secrecy purposes

The aforementioned domain size represents the 100% relative domain sizing, symbolized by the red dot. The domain was scaled along its 3 axis to create larger and smaller domains to compare to.

The domain sizing we used did prove independency of the solution, and optimization toward computing efficiency since it's one of the smallest domain (and smallest mesh) that reach an independent result. However, larger domains did prove some advantages such as a faster convergence and a better solution stability, leading to the use of a 110% or 120% size domain for some computing cases (e.g. aero map generation).

To each boundary of the domain is affected a boundary condition.

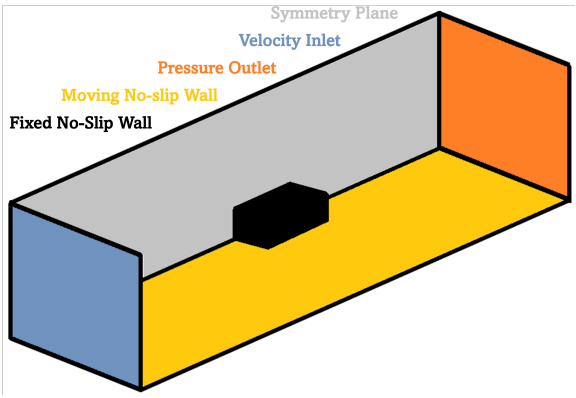

Figure 7: Boundary conditions of the domain and geometry (without slip walls)

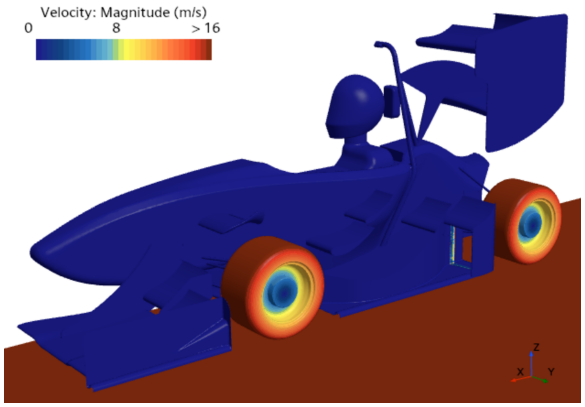

Figure 8: Velocity-defined no-slip walls and ground/wheel coherence

The velocity condition of the inlet is parameterized to allow for easier modification of the airspeed of each case. The case simulation uses a symmetry condition to divide by half the domain size and overall computing time is reduced by 50-60%. The ground is a no-slip wall defined by a vector to replicate a ground moving under the car, affecting primarily the ground effect, and is tied to the airspeed value. All of the car parts (with the exception of the radiator) are also no-slip walls. A rotation is affected to the wheels to simulate rolling wheels, improving the accuracy of wheel wake effects. The box is closed by slip walls.

Automated Meshing Pipeline

To transform a continuous domain into a discrete domain, we have to divide it into smaller cells connected by nodes and faces. These cells are the exact points where the RANS physics equation will be solved. However, this subdivision of the domain must be done cleverly as to not yield physically incoherent results.

To achieve a greater mesh quality, we will use 2 different meshing techniques. We will first create a surface mesh of the domain to repair any CAD imperfection and provide a airtight base to then run an automated volume mesh algorithm with specified parameters.

Surface Meshing and Airtight Wrapper

The surface mesher, otherwise called a surface wrapper in StarCCM+, aims to re-triangulate the imported CAD parts to create a clean surface base to use for the volume mesh. It also aims towards removing small features and closing small gaps due to CAD modeling errors.

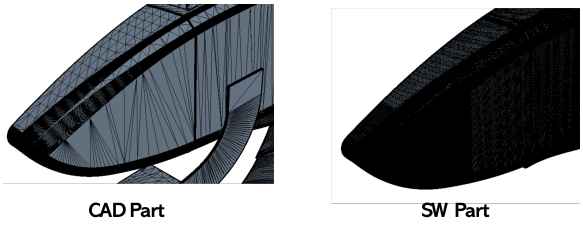

Figure 9: Comparison between the original CAD Part triangulation and the post-Surface Wrapper part triangulation

The Surface Wrapper operation is separated in 4 part groups in order to shorten the meshing wall time by not re-meshing parts that have not been modified from an iteration to another. The minimum size allowed for a surface element is 0.5 millimeters with the target surface size being 20 millimeters.

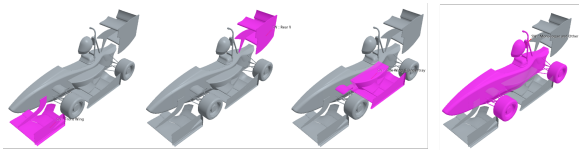

Figure 10: Four different groups of Surface Wrapper

Each parameter of each subgroup is fine tuned to approach the original geometry input as closely as possible. Conditions of no-contact between parts are created to avoid bridging between parts that would lead to a lower fidelity geometry.

Automated Volume Mesh

Once a high-fidelity surface has been output from the Surface Wrapper operations, and once they have been subtracted from the domain, we set up the Automated Mesh algorithm that will generate a Volume Mesh from a defined set of parameters.

Specifically, we use a Trimmed Cell Mesher that trims the cell in contact with a surface until a certain threshold is achieved for a minimum

size. This meshing technique allows for very regular cells, but lacks precision around the surface if transition layers aren't used between the trimmed cells and the surface, generally PRISM layers for boundary layer meshing.

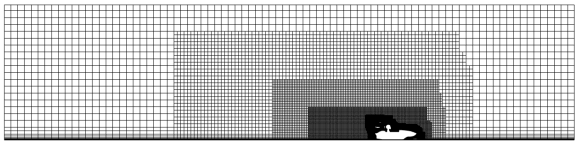

Figure 11: Side view of the mesh over the symmetry plane (y = 0.0 mm)

Different refinement methods are used, whether they're surface or volume controlled. Wake refinement is managed through several refinement boxes rearwards of the car to force a progressive anisotropic change in cell size, to better capture the strong effects tied to wake and induced drag. A curvature refinement is also included to better model the wing-bounded flows at their leading edge.

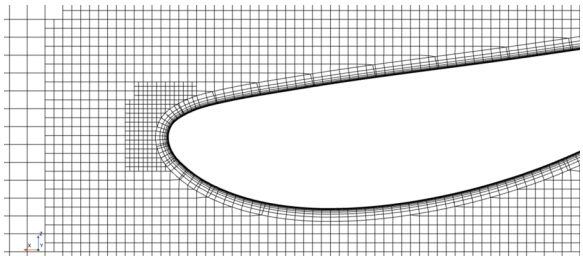

Figure 12: Boundary layer and wing meshing

The PRISM-layer mesher is tuner for each main wing of the prototype according to their respective length and boundary layer thickness to achieve a wall $y^+ < 1$ on all surfaces of the prototype. Special parameters are set to manage the increased boundary layer size around the wheels.

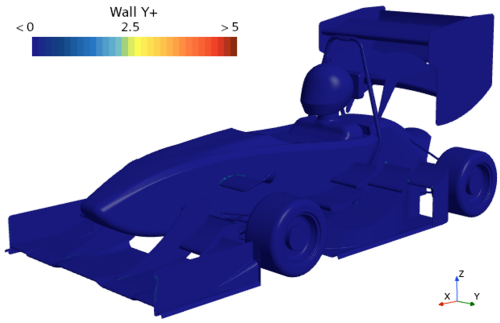

Figure 13: Visualization of the Y+ over the car and its symmetry

Physics Equation and Solver

Depending on the problem, multiple physics continua exist to study different types of cases with different sets of equations. It is important to select the right equations that will allow for the calculation of wanted quantities.

In our case, since we're trying to only model subsonic aerodynamics around an object with no density variation and no chemical or thermal effects, we will stick to "simple" equations for fluid mechanics calculations.

Application of Navier-Stokes equations to CFD

The equations of Navier-Stokes are the fundamental equations that govern any newtonian fluid flow. They're a variation of Newton's second law applied to an elementary volume of fluid coupled to an Eulerian inviscid formulation, introducing a stress tensor proportional to velocity gradients (or rate of strains tensor [6]) to account for viscous effects [7]. It is defined as follows in the Einstein-index convention.

$$\rho \frac{D\mathbf{u}}{Dt} = \rho \left(\frac{\partial \mathbf{u}}{\partial t} + (\mathbf{u} \cdot \nabla)\mathbf{u} \right) = \underbrace{-\nabla \tilde{p}}_{\text{pressure forces}} + \underbrace{-\tilde{\rho}\mathbf{g}}_{\text{gravity forces}} + \underbrace{-\nabla \cdot \tilde{\boldsymbol{\tau}}}_{\text{viscosity forces}}$$

Those equations, although very versatile, are computationally very expensive and can't be applied to industrial fluid cases. Reynolds offered the hypothesis that velocity and pressure gradients could be decomposed into a mean value and a fluctuation over the domain, theorizing an equation of mean motion at every point leading to the genesis of the Reynolds-Averaged Navier-Stokes (RANS) equations [8].

$$\rho \left(\frac{\partial \overline{U}_i}{\partial t} + \frac{\partial \overline{U}_i \, \overline{U}_j}{\partial x_j} \right) = - \frac{\partial \overline{P}}{\partial x_i} + \frac{\partial}{\partial x_j} \left(\overline{\tau}_{ij} - \rho \, \overline{u_i' u_j'} \right)$$

where $\rho \, \overline{u_i' u_j'}$ is the Reynolds tensor, symbolizing additional stress from turbulence agitation.

$$\rho \, \overline{u_i' u_j'} = \rho \begin{pmatrix} \overline{u'^2} & \overline{u'v'} & \overline{u'w'} \\ \overline{u'v'} & \overline{v'^2} & \overline{v'w'} \\ \overline{u'w'} & \overline{v'w'} & \overline{w'^2} \end{pmatrix}$$

The diagonal components $\rho \, \overline{u_i'^2}$ are generally called normal stresses while the extra diagonal components are called shear stresses. For laminar flows, shear stresses are zero and the RANS equations present 4 equations (momentum, conservation of mass) for 4 unknowns (p and u_i) : the problem is closed an can be solved.

However, for turbulent flows, shear stresses exist and can't be disregarded, leading to an open problem with 4 equations for 10 unknown variables. It's known as the closure problem.

Over the last decades, closing these equations has been a great subject in fluid mechanics, with Boussinesq [9] formulating the first explicit closure, discovering quantities such as the eddy viscosity to create a Reynolds-stress transport model. Prandlt [10] with the help of Boussinesq's work theorized a hierarchy in the governing equations, modeling turbulence within boundary layers through his mixing-length theory.

The current formulations and turbulence models in use have proved good correlation to experimental data and are generally a solid basis to study aerodynamics of an FSAE Car, in particular the Menter SST k-ω model [11] that relies on a blend of the k-ϵ and k-ω turbulence models, adapted for high gradients within the boundary layer as well as freestream flows with a reasonable computational cost. The equations involved are :

$$\frac{\partial(\rho k)}{\partial t} + \frac{\partial(\rho U_j k)}{\partial x_j} = P_k - \beta^* \, \rho k \omega + \frac{\partial}{\partial x_j} \left[(\mu + \sigma_k \mu_t) \, \frac{\partial k}{\partial x_j} \right]$$

$$\frac{\partial(\rho \omega)}{\partial t} + \frac{\partial(\rho U_j \omega)}{\partial x_j} = \alpha \, \frac{\omega}{k} \, P_k - \beta \, \rho \omega^2 + \frac{\partial}{\partial x_j} \left[(\mu + \sigma_\omega \mu_t) \, \frac{\partial \omega}{\partial x_j} \right] + 2 \, (1 - F_1) \, \rho \, \sigma_{\omega 2} \, \frac{1}{\omega} \, \frac{\partial k}{\partial x_j} \, \frac{\partial \omega}{\partial x_j}$$

For our case study, we will use RANS equations coupled with a Menter's SST turbulence model since it's the most suited for our case study involving high-shear flows in boundary layers as well as free-shear flows.

Solver Parameters and Setup

For this steady-state case, we will use a coupled implicit solver, with a fixed Courant-Friedrichs-Lewy number, a MUSCL 3rd order discretization and a Roe scheme (no blending) for inviscid fluxes.

The coupled solver ensures a strong coupling of the conservative variables in incompressible flows that outputs faster and smoother convergence than segregated schemes. Implicit time stepping limits CFD dependance while providing a much more stable solver that reaches convergence faster. [12]

The MUSCL 3rd-order discretization allows for a better precision when solving the pressure gradients, vortices and boundary layers to limit oscillations at convergence and increase resolution of the solution. It also prevents excessive diffusion in highly separated regions. [13]

The Roe scheme ensure the respect of the wave structures of the Euler formulation, generally for transonic flows and shock capturing purposes. In subsonic cases, it helps with forces prediction and pressure distribution prevision and offers a better accuracy for highly accelerated flows in external aero conditions. [14]

Those parameters build a model that offers a robust convergence with high accuracy and low noise, ensuring sharpness and determinism of the solution to a high degree.

Results & Analysis

Formule ETS' 2025 prototype, DELTA-25, was studied for speeds comprised between 4 meters per second and 32 meters per second. Ride heights for front and rear axle are within the 15 millimeters to 40 millimeters range.

Validation

Convergence of the Solution

Mesh and Domain Independence

Wind-Tunnel Validation

NB : Precise validation methodology involving Wind Tunnel Testing is the subject of the FETS-2025-01 reference [15].

Track Data Correlation

Conclusion

This model, although very simple, proved to be reliable to study the effects of new aerodynamic devices on a FSAE prototype. It's also versatile, as it can be easily modified to simulate wind tunnel condition by disabling wheel rotation and ground movement, as well as react to different speeds. The symmetry can be disabled too to study the yaw sensitivity of the aero package.

The slight deviation in wind tunnel validation could be explained by a minor over simplification of the geometry, however a 5% constant deviation is a remarkable result considering the involved methodologies and will be considered enough for further studies.

Recommendation

We recommend, as many of the aerodynamic judges have, to keep in mind that aerodynamic effects take an increased importance during cornering situation, where the goal is to maximize the lateral force produced by the tire through increased downwards force, leading to a higher lateral acceleration and higher cornering speed.

This straight line model takes into account various effects through precise parameterization, but lacks account of any non-symmetrical behaviors to reduce computing time and increase design productivity which should be studied to conclude on the reliability of straight line aerodynamics for FSAE race cars.

On another hand, being a steady-state model, all the transient effects are averaged and erased from analysis outside of the occasional steady-state stabilization oscillations. We strongly recommend a study on transient effects of Formule ETS' car to determine its influence on overall aerodynamics.

References

1. H. Perrin, *Modeling Cornering Aerodynamics - A Review*. Formule ETS, 2024.
2. H. Perrin and E. Houri, *Aerodynamic Simulation of a FSAE Open-Wheel Car During Cornering*. Formule ETS, 2024.
3. W. K. Liu, X. Li, and K. Park, "Eighty years of the finite element method: Birth, evolution, and future," *Archives of Computational Methods in Engineering*, vol. 29, no. 4, 2022.
4. M. D. Griffin, R. Diwakar, J. Anderson, J. D., and E. Jones, "Computational fluid dynamics applied to flows in an internal combustion engine," in *AIAA 16th Aerospace Sciences Meeting*, 1978. AIAA Paper 78-57.
5. C. Shaw, "Predicting vehicle aerodynamics using computational fluid dynamics - a user's perspective," *SAE Technical Paper*, vol. 880455, p. 16, 1988.
6. G. G. Stokes, "On the theories of the internal friction of fluids in motion, and of the equilibrium and motion of elastic solids," *Transactions of the Cambridge Philosophical Society*, vol. 8, pp. 287–319, 1845.
7. C. L. M. H. Navier, "Mémoire sur les lois du mouvement des fluides," *Mémoires de l'Académie Royale des Sciences de l'Institut de France*, vol. 6, pp. 389–440, 1823.
8. O. Reynolds, "On the dynamical theory of incompressible viscous fluids and the determination of the criterion," *Philosophical Transactions of the Royal Society of London. Series A*, vol. 186, pp. 123–164, 1895.
9. J. Boussinesq, *Essai sur la théorie des eaux courantes*, vol. 23 of *Mémoires présentés par divers savants à l'Académie des Sciences de l'Institut National de France*. Paris: Imprimerie nationale, 1877.
10. L. Prandtl, "Über flüssigkeitsbewegung bei sehr kleiner reibung," in *Verhandlungen des III. Internationalen Mathematiker-Kongresses*, (Heidelberg), pp. 484–491, B. G. Teubner, 1904.
11. F. R. Menter, "Two-equation eddy-viscosity turbulence models for engineering applications," *AIAA Journal*, vol. 32, no. 8, pp. 1598–1605, 1994.
12. A. Jameson, W. Schmidt, and E. Turkel, "Numerical solution of the Euler equations by finite volume methods using runge–kutta time stepping schemes," in *14th Fluid and Plasma Dynamics Conference*, AIAA, 1981. AIAA Paper 81-1259.
13. B. van Leer, "Towards the ultimate conservative difference scheme. v. a second-order sequel to godunov's method," *Journal of Computational Physics*, vol. 32, no. 1, pp. 101–136, 1979.
14. P. L. Roe, "Approximate riemann solvers, parameter vectors, and difference schemes," *Journal of Computational Physics*, vol. 43, no. 2, pp. 357–372, 1981.
15. H. Perrin, *Wind Tunnel Validation of an Open-Wheel FSAE Car*. Formule ETS, 2025.

Definitions, Acronyms, Abbreviations

CAD	Computer Assisted Design
CFD	Computational Fluid Dynamics
CSM	Cornering Simulation Model
HPC	High Performance Computing
FEA	Finite Element Analysis
FSAE	Formula Society of Automotive Engineers
RANS	Reynolds-Averaged Navier–Stokes
SLSM	Straight Line Simulation Model

Contact Information

Hugues PERRIN, M.Sc
contact@huperrin.com

Eline HOURI, M.Eng
e.houri.formule.ets@gmail.com